Editors' Suggestion

Dynamics of Vitrimers: Defects as a Highway to Stress Relaxation

Simone Ciarella,[1,*] Francesco Sciortino,[2] and Wouter G. Ellenbroek[1,3,†]
[1]Department of Applied Physics, Eindhoven University of Technology, Postbus 513, NL-5600 MB Eindhoven, Netherlands
[2]Department of Physics and CNR-ISC, Sapienza Universitá di Roma, Piazzale Aldo Moro 2, I-00185 Roma, Italy
[3]Institute for Complex Molecular Systems, Eindhoven University of Technology, Postbus 513, NL-5600 MB Eindhoven, Netherlands

(Received 29 March 2018; revised manuscript received 22 June 2018; published 31 July 2018)

We propose a coarse-grained model to investigate stress relaxation in star-polymer networks induced by dynamic bond-exchange processes. We show how the swapping mechanism, once activated, allows the network to reconfigure, exploring distinct topological configurations, all of them characterized by complete extent of reaction. Our results reveal the important role played by topological defects in mediating the exchange reaction and speeding up stress relaxation. The model provides a representation of the dynamics in vitrimers, a new class of polymers characterized by bond-swap mechanisms which preserve the total number of bonds, as well as in other bond-exchange materials.

DOI: 10.1103/PhysRevLett.121.058003

Vitrimers, an exciting new class of polymer networks, are unique in their ability to interpolate between the two conventional classes of polymer, thermoplastics and thermosets [1]. The first can be reshaped at will but are sensitive to being weakened by contact with solvents, while the latter are insoluble but cannot be reshaped after the cross-linking process. In vitrimers, a connectivity-preserving bond-exchange mechanism [2–5] with well-controlled exchange rate makes the cross-links dynamic. At low rates, they perform like thermosets, while at high rates, they are malleable like thermoplastics. Unlike permanently cross-linked elastomers or gels, these bond swaps allow vitrimers to release internal stresses without losing shape. Their versatility shines, particularly in smartly designed materials, where bond swapping provides a welding strategy [6], or responsiveness to light, *p*H, voltage, metal ions, redox chemicals, and mechanical stimuli [7–9].

The unusual molecular interaction in vitrimers renders current theories of polymer performance of limited use. Neither a conventional static model nor a fully dynamic one can coherently address the exchange dynamics. At the atomistic level, exchange reactions can be effectively modeled using reactive force fields [10]. This gives a detailed picture of a single exchange event but does not provide large enough time and length scales to assess macroscopic properties. To get to macroscopic scales, a coarse-grained model that captures the network-topology aspects of the exchange reactions is needed.

In recent years, scientists have developed different numerical models to study exchange materials [11–14], embedding Monte Carlo hopping moves into hybrid molecular dynamics (MD) or Monte Carlo simulations to reproduce bond swaps. In this Letter, we study a vitrimer model consisting of associative star polymers using a three-body potential to reproduce bond-exchange dynamics with a controllable rate [15], avoiding the need for hybrid features. Using molecular dynamics simulations to obtain the stress relaxation modulus, we verify the expected transition from solidlike to liquidlike long-time behavior upon increasing the bond-exchange rate [16]. More importantly, we uncover a dramatic difference in stress relaxation that arises from the molecular topology. In close connection to recent work that demonstrated how loops affect equilibrium elastic properties [17], we show that networks made from building blocks that allow loop formation via bond exchange relax stresses much faster than systems made from loop-preventing building blocks, even when the bond-exchange rates are the same. Thus, the slow relaxations that characterize swapping vitrimers [18] can be controlled not only through the swap rate but also through defect formation. In this sense, loop defects serve as highways to stress relaxation, giving faster self-healing and better malleability and recyclability [4,13]. Combining this effect with an accurate choice of the network topology, we can imagine synthesizing a material which is not only stable as thermosets and malleable as thermoplastics but also tougher than either because it can relax stresses in a controllable way, while having improved structural integrity compared to materials toughened via other mechanisms such as fully reversible cross-linking [19] or sacrificial bonds [20].

Modeling vitrimers.—We focus our simulations on networks built from binary mixtures of eight-arm star polymers. Each arm terminates with a reactive site which can be of two different types labeled red and blue [see Fig. 1(a)]. This effectively captures what happens in vitrimers that rely on covalent association of two different moieties via, e.g., ester bonds [4,5], in which case, the end types represent carboxyl and hydroxyl groups, respectively. Star-shaped monomers are widely used polymeric building blocks,

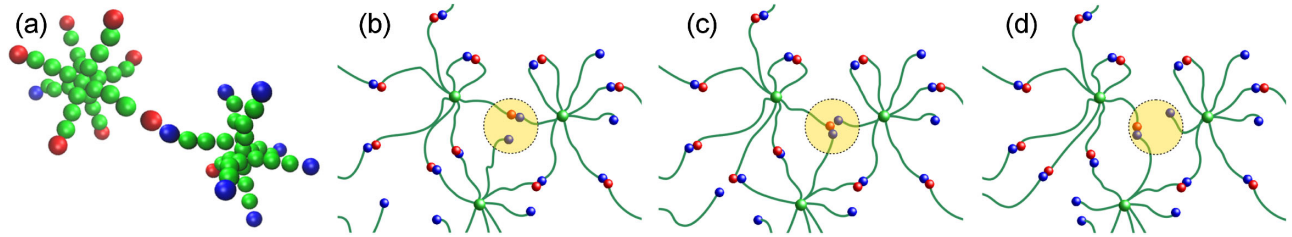

FIG. 1. (a) Star-shaped monomers forming a swappable covalent bond (red and blue). (b)–(d) Sketch of a swap event: Red-blue bonds can swap, while green beads are permanent links (the centers of the stars). The swap reaction modifies the topology of the network. Its rate is catalytically controlled in real systems: here it is modelled by tuning the energy barrier. In states (b) and (d), there is only a two-body energy term ($\approx -\epsilon$) due to the highlighted bond. In state (c), there are two two-body energy terms ($\approx -2\epsilon$) and one three-body contribution ($\approx +\lambda\epsilon$). If $\lambda = 1$, the three-body term compensates exactly the formation energy of the second bond, effectively flattening out the energy barrier.

e.g., for dendrimers and tetra-PEG hydrogels [21,22]. They are a versatile basis for covalent adaptive networks, with controlled connectivity and architecture [2].

We coarse grain the star polymer as a sequence of beads and harmonic springs [23] with an equilibrium bond length of 1 nm, which is our unit of length. The beads shown in green in Fig. 1(a), thus, represent Kuhn segments consisting of roughly eight carbon atoms. Masses, energies, and times are expressed in units $[m] = 100$ u, $[E] = k_B \times 300$ K, and $[\tau] = 6.33$ ps, respectively. All pairs of beads interact via a purely repulsive Weeks-Chandler-Andersen potential ($\sigma = 1$ nm) [24].

Modeling swappable covalent bonds using potentials requires care. They must enforce single red-blue bonds without clustering, contain a parameter to tune the swap rate, and the bonds they provide must be thermally stable. To this end, we use a combination of two-body and three-body interactions as proposed in Ref. [15]. The two-body term is a generalized Lennard-Jones potential acting only between red-blue pairs,

$$v_{ij}(\vec{r}_{ij}) = 4\epsilon\left[\left(\frac{\sigma}{r_{ij}}\right)^{20} - \left(\frac{\sigma}{r_{ij}}\right)^{10}\right], \quad r < r_{\text{cut}}. \tag{1}$$

With $\sigma = 0.5$ nm and $\epsilon = 100 k_B T$, the v_{ij} provide a covalentlike bond that is stable against thermal fluctuations. We fix $r_{\text{cut}} = 2.5\sigma$. The three-body term is rewritten in terms of how the interaction between particles i and j is affected by the presence of other particles k that are within range of particle i,

$$v_{ijk}^{(3b)} = \lambda\epsilon\hat{v}_{ij}^{(2b)}(\vec{r}_{ij})\hat{v}_{ik}^{(2b)}(\vec{r}_{ik}), \tag{2}$$

where $\lambda \geq 1$ is the three-body scaling parameter, and $\hat{v}_{ij}^{(2b)}$ is defined as

$$\hat{v}_{ij}^{(2b)}(\vec{r}_{ij}) = \begin{cases} 1, & r \leq r_{\text{min}}, \\ -\frac{v_{ij}(\vec{r}_{ij})}{\epsilon}, & r > r_{\text{min}}, \end{cases} \tag{3}$$

where r_{min} is the position of the minimum in Eq. (1). Because it is formulated in terms of the attractive part of the two-body term, this three-body potential compensates the pair energy that would be gained by two simultaneous red-blue bonds so that all intermediate states encountered during a swap event are similar in potential energy. This flat energy landscape is the defining feature of the method, as illustrated in Figs. 1(b)–1(d). The three-body term automatically enforces the single bond per reactive site since it gives a strong repulsion when more than three reactive sites are close. The parameter λ sets the energy barrier for a swap rearrangement ΔE_{sw}. To first approximation, $\beta\Delta E_{\text{sw}} \equiv \beta\epsilon(\lambda - 1) = 100(\lambda - 1)$.

While three-body interactions are generally expensive in simulations, Eq. (2) requires only small additional numerical effort compared to a standard two-body potential because it is a combination of the existing two-body terms.

Numerical approach.—We use the HOOMD-blue package [25,26] to do molecular dynamics simulations on Graphic Processing Units. For the three-body potential, we developed a HOOMD-blue module named "RevCross." This implementation allows us to gather sufficient statistics for evaluating the stress relaxation in systems of $N \approx 50\,000$ beads (≈1500 star polymers). We use a time step size $dt = 10^{-3}[\tau]$. To provide a reservoir of open endings that can initiate a swap event, we use a nonstoichiometric mixture of different star endings, following the chemistry behind vitrimers. We exploit two different mixtures to assess the role of defects (loops) in the stress relaxation.

We focus on the type of defects known as primary loops, in which two endings of the same star are bonded together. These are the most important for the static elastic properties [17]. First, we employ a defect-free mixture (DFM) composed of $N_A = 900$ eight-arm star polymers whose endings are only type A and $N_B = 600$ stars with only B-type ends. Since A—B bonds are allowed, primary loops are prevented. Later, we present results on a defect-allowing mixture (DAM) which contains $N_A = 950$ stars with seven A-type endings and a single B-type ending, and $N_B = 550$ stars with the numbers reversed. These values of N_A and N_B make the total number of red and blue beads identical in both mixtures. Since the red-blue bonds are much stronger than $k_B T$, all 4800 B-type ends will form a

bond, leaving 2400 free A-type ends available to initiate swap events. The large number of arms is used in order to have a network that behaves like a solid without applying any (osmotic) stretching. Both networks are equilibrated in periodic cubic boxes of size $L = 40$ nm corresponding to a packing fraction $\phi \approx 0.3$. This corresponds to 2.2 times the overlap concentration, so the stars can easily form a network, but it is low enough to avoid any glassy dynamics. In the Supplemental Material [27], we demonstrate that indeed there is no caging or segmental slowing-down at this density, so that the polymer arms are mobile enough to initiate bond swaps [27]. For both DFM and DAM mixtures, we generate $m = 100$ independent network topologies.

Stress relaxation.—We perform stress relaxation calculations. Rather than doing out-of-equilibrium MD to calculate the stress $\sigma(t)$ after a step strain, we exploit the widely used autocorrelation method

$$G(t) \approx C(t) \equiv \frac{V}{k_B T} \langle \overline{\sigma_{yz}(t)\sigma_{yz}(0)} \rangle \tag{4}$$

in the nVT ensemble where we imposed the number of stars n, the volume V, and the temperature T. The bar and brackets denote averaging over time and ensemble, respectively. To calculate the instantaneous stress $\sigma(t)$, we have to add terms that arise from the three-body potential to the standard (pair-based) virial expression. In the Supplemental Material [27], we derive these terms from the thermodynamic definition of stress.

The stress autocorrelation function is often assumed to be equal to the stress relaxation $G(t)$, but it was recently pointed out that the equality holds only in liquids [33,34]. The correct way to define the stress relaxation would be

$$G(t) = \begin{cases} C(t), & \text{liquids}, \\ C(t) + G_{\text{eq}} - C_\infty & \text{solids}, \end{cases} \tag{5}$$

where G_{eq} is the shear modulus, and C_∞ is the long-time asymptote of $C(t)$ [so $C_\infty \propto \langle \bar{\sigma} \rangle^2$]. Thus, the stress autocorrelation function $C(t)$ and the stress relaxation modulus $G(t)$ always coincide in the liquid phase, but when the system rigidifies, $C(t)$ shifts from $G(t)$ by a constant [33]. Still, one can distinguish a solid from a liquid using the limiting behavior of $C(t)$, even in a finite ensemble. The reason this works is that the only way to have $C_\infty = 0$ is when $\bar{\sigma} = 0$ for every configuration, which happens only for liquids. Furthermore, the constant $C_\infty = 0$ goes to zero for self-assembled networks through the average over different architectures [12]. For this reason, $C(t) = G(t)$ in our calculations.

Swap-driven transition without loops.—The stress relaxation for the DFM system is reported in Fig. 2(a). We define τ_{net} as roughly the time that it takes for a solid network to reach its elastic plateau, $\tau_{\text{net}} \approx 5$ ns. At short times ($t < \tau_{\text{net}}$), the stress relaxation is dominated by chain motion [35]. We refrain from fitting a power law to this regime because the arms of the star polymers are too short to make this feasible. All curves coincide until this timescale because swapping is slow and the network topology is essentially fixed. Then, the gel starts sustaining the stress and a plateau in $G(t)$ appears. If the swap move has a large energy barrier ($\beta \Delta E_{\text{sw}} > 50$), the topology remains fixed, and the plateau extends beyond times reachable by simulation. If, instead, the gel rearranges through bond-swap moves, we observe a second relaxation, the hallmark of transient networks [12–14,36]. We conclude that when there is no activation barrier, swaps make DFM liquid at $\tau_{\text{liq}}^{\text{DFM}} \approx 20$ μs, where we picked $G(\tau_{\text{liq}})/G(0) \equiv 10^{-4}$.

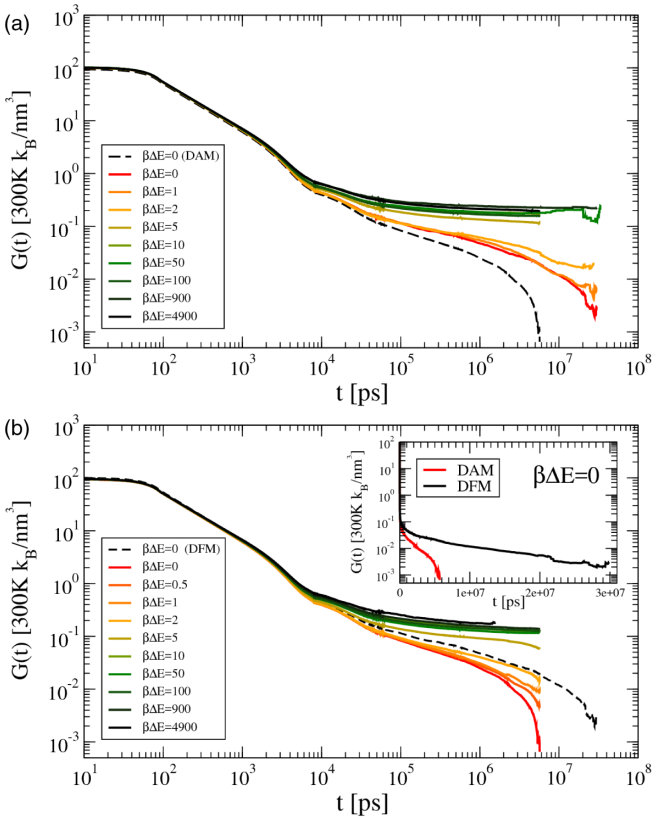

FIG. 2. (a) Stress relaxation for the DFM for a range of swap barrier values (DAM data are shown as a dashed line for comparison). (b) Stress relaxation for the DAM, with DFM data shown as a dashed line for comparison. After the first regime of relaxation due to chain rearrangement, a solid plateau is approached, which is slightly higher than the $\rho k_B T = 0.075[k_B T/\text{nm}^3]$ one would expect for ideal rubbers obeying Kuhn theory. For low enough energy barriers, swap rearrangements trigger a second relaxation. This network relaxation is an order of magnitude faster with defects than without. The small time damped oscillation is suppressed by plotting only the local maxima for $t \leq 1000$ ps. Inset: DAM and DFM comparison on a linear time axis.

Swap-driven transition with loops.—The stress relaxation for the DAM system is reported in Fig. 2(b). After chain

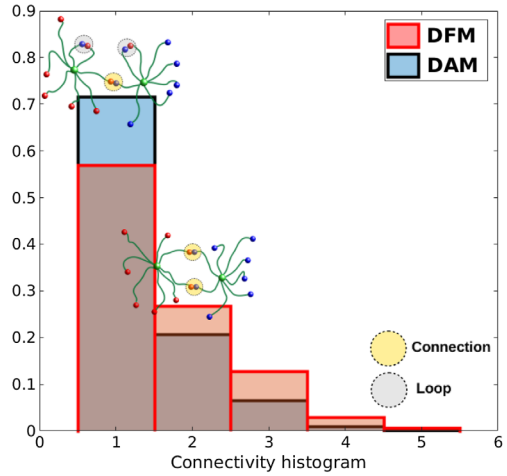

FIG. 3. Histogram of the number of connections between connected stars for both mixtures. In the DAM (blue), the presence of loops causes the average number of connections between stars to be lower. This reduces redundancy and thereby increases the chance that a single swap even will disconnect two stars, which speeds up stress relaxation.

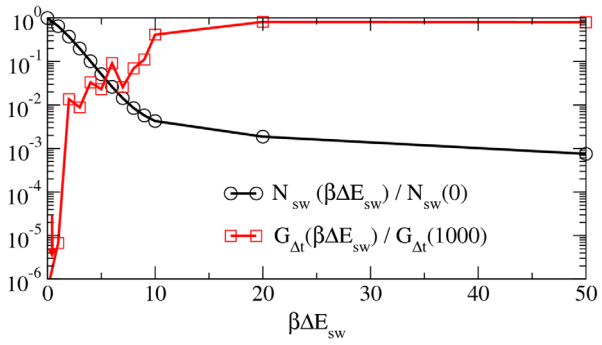

FIG. 4. Normalized number of swaps (black) and stress relaxation (red) as a function of the swap energy barrier $\beta\Delta E_{\mathrm{sw}}$ for the DAM system. The fluid-solid transition happens when the barrier is $10k_BT$. Note that between 10 and $20k_BT$, the number of swaps becomes so small that the system ceases to be ergodic on the timescale of the simulation. While this estimate refers to the simulation time, the expected exponential growth with $\beta\Delta E$ of the single swap event suggest that already $\beta\Delta E \approx 20$ is a robust estimate for ergodicity loss even in the real world. Data are taken at $\Delta t = 10^7$ ps.

relaxation, the solid plateau is approached only by the fixed networks, while the swapping ones keep relaxing all of their stress. In this mixture, bond swapping contributes to stress relaxation on shorter timescales. In marked contrast with the system without loop defects, the final stress relaxation is now 10 times faster, $\tau_{\mathrm{liq}}^{\mathrm{DAM}} \approx 0.1\tau_{\mathrm{liq}}^{\mathrm{DFM}} \approx 2$ μs. The swapping gel with defects behaves essentially like a viscous liquid.

To rule out that the faster stress relaxation is caused by structural quantities unrelated to loop defects, we verified that all 2400 possible bonds formed in both mixtures and that the number of swap events are similar in both. Finally, we checked that the DAM mixture indeed formed loop defects and found that typically between $1/5$ and $1/3$ of all bonds in this mixture are primary loops connecting two arms of the same star.

The conclusion is that the fast stress relaxation of the defect-allowing mixture is caused by "defected" configurations. Whenever an intrastar bond that was carrying stress is swapped with an arm on the same star to form a defect, it ceases to support stress, giving rise to dissipation. This consistently leads to fewer redundant connections between stars, as we show in Fig. 3, which, in turn, makes the fraction of swap events that actually detach two stars even larger, leading to more relaxation per event. Given that the swap rate is similar for the two mixtures, this means the defects act as a highway to stress relaxation.

Discussion.—We have shown the effectiveness of MD simulations in the study of bond-swapping systems. The employed three-body potential turns bond-swap events into a continuous process: Free binding sites approach an existing bond via a tunable barrier, and after the exchange, the unbound partner leaves via the same pathway. The computational effort of evaluating a three-body interaction is partly mitigated by defining it in terms of pair forces which had to be computed anyway. Compared to Monte Carlo moves for bond exchanges, our approach has the advantage that dependence of exchange probability on physical parameters such as the bond force arises naturally and does not have to be manually added into an acceptance criterion.

Figure 4 shows the swap rate decreases by 2 orders of magnitude when $\beta\Delta E_{\mathrm{sw}}$ is increased from zero to 6, correlated with the rise of the elastic plateau in the stress relaxation modulus $G(t)$ measured at the simulation limit $\Delta t = 10^7$ ps. Thus, $\beta\Delta E_{\mathrm{sw}}$ controls the solid-liquid transition or topological glass transition in the same way as catalyst concentration or temperature in experiments.

Applying this method to two different mixtures, we demonstrate the importance of topological considerations for stress relaxation, extending recent insights into the effect of looplike defects on static elastic properties [17,37]. With the same number of swapping events, our primary-loop-free mixture of star polymers relaxes stress much more slowly than the loopy mixture of otherwise similar star polymers.

We stress the peculiar role for doubly connected stars in these networks: For the static modulus, there is little difference between a single or double polymer bridge between two star centers, as each bridge in a second-order loop is about half as effective as a single bridge [17]. When it comes to relaxing stresses via swapping, however, the doubly connected stars contribute much more slowly since the force between them will only be relaxed away after both bonds have undergone a swap.

Interestingly, we found that we can exert some control over how many loops are formed (and, thus, over stress relaxation) in the defect-allowing mixture by way of excluded volume interactions, temperature, and deformation, as we show in

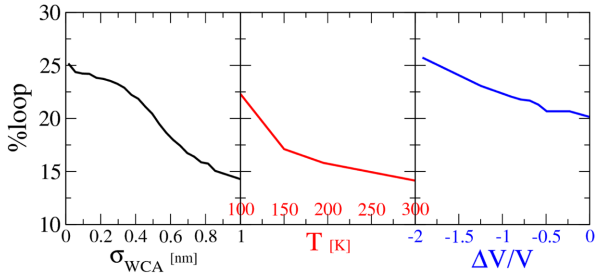

FIG. 5. We can control the number of loop defects by inflating the monomers (black), increasing temperature (red), or volumetric compression (blue).

Fig. 5. In addition, this control over topology also paves the way for a novel type of elastomer with switchable elastic properties: Quenching a vitrimer from an equilibrated bond-swapping state down to a state in which no swaps occur, the number of loops is frozen, which fixes the elastic modulus [17]. The same material could later be annealed under different conditions with different loop statistics, so that the modulus can be switched. This is in marked contrast to usual thermoset elastomers, which have their loop content fixed at synthesis time [37].

In summary, our results suggest that novel vitrimer systems can be designed explicitly considering defects as a means to control mechanical properties. This class of polymeric materials will then, on top of their recyclability and their remarkable ability to recover their initial properties after remolding, also become mechanically tunable.

We are grateful to Hans Heuts and Cornelis Storm for helpful comments.

*s.ciarella@tue.nl
†w.g.ellenbroek@tue.nl

[1] M. Rubinstein and R. H. Colby, *Polymer Physics* (Oxford University Press, New York, 2003), Vol. 23.
[2] C. J. Kloxin and C. N. Bowman, Chem. Soc. Rev. **42**, 7161 (2013).
[3] W. Denissen, J. M. Winne, and F. E. Du Prez, Chem. Sci. **7**, 30 (2016).
[4] D. Montarnal, M. Capelot, F. Tournilhac, and L. Leibler, Science **334**, 965 (2011).
[5] M. Capelot, D. Montarnal, F. Tournilhac, and L. Leibler, J. Am. Chem. Soc. **134**, 7664 (2012).
[6] E. Chabert, J. Vial, J.-P. Cauchois, M. Mihaluta, and F. Tournilhac, Soft Matter **12**, 4838 (2016).
[7] Q. Chen, X. Yu, Z. Pei, Y. Yang, Y. Wei, and Y. Ji, Chem. Sci. **8**, 724 (2017).
[8] Z. Yang, Q. Wang, and T. Wang, ACS Appl. Mater. Interfaces **8**, 21691 (2016).
[9] A. R. de Luzuriaga, J. M. Matxain, F. Ruipérez, R. Martin, J. M. Asua, G. Cabañero, and I. Odriozola, J. Mater. Chem. C **4**, 6220 (2016).
[10] A. C. Van Duin, S. Dasgupta, F. Lorant, and W. A. Goddard, J. Phys. Chem. A **105**, 9396 (2001).
[11] B. Oyarzún and B. M. Mognetti, J. Chem. Phys. **148**, 114110 (2018).
[12] J. P. Wittmer, I. Kriuchevskyi, A. Cavallo, H. Xu, and J. Baschnagel, Phys. Rev. E **93**, 062611 (2016).
[13] E. B. Stukalin, L.-H. Cai, N. A. Kumar, L. Leibler, and M. Rubinstein, Macromolecules **46**, 7525 (2013).
[14] F. Smallenburg, L. Leibler, and F. Sciortino, Phys. Rev. Lett. **111**, 188002 (2013).
[15] F. Sciortino, Eur. Phys. J. E **40**, 3 (2017).
[16] F. Snijkers, R. Pasquino, and A. Maffezzoli, Soft Matter **13**, 258 (2017).
[17] M. Zhong, R. Wang, K. Kawamoto, B. D. Olsen, and J. A. Johnson, Science **353**, 1264 (2016).
[18] L. Rovigatti, G. Nava, T. Bellini, and F. Sciortino, Macromolecules **51**, 1232 (2018).
[19] Z. S. Kean, J. L. Hawk, S. Lin, X. Zhao, R. P. Sijbesma, and S. L. Craig, Adv. Mater. **26**, 6013 (2014).
[20] E. Ducrot, Y. Chen, M. Bulters, R. P. Sijbesma, and C. Creton, Science **344**, 186 (2014).
[21] T. Sakai, T. Matsunaga, Y. Yamamoto, C. Ito, R. Yoshida, S. Suzuki, N. Sasaki, M. Shibayama, and U. I. Chung, Macromolecules **41**, 5379 (2008).
[22] T. Matsunaga, T. Sakai, Y. Akagi, U.-i. Chung, and M. Shibayama, Macromolecules **42**, 1344 (2009).
[23] K. Kremer and G. S. Grest, J. Chem. Phys. **92**, 5057 (1990).
[24] J. D. Weeks, D. Chandler, and H. C. Andersen, J. Chem. Phys. **54**, 5237 (1971).
[25] J. A. Anderson, C. D. Lorenz, and A. Travesset, J. Comput. Phys. **227**, 5342 (2008).
[26] J. Glaser, T. D. Nguyen, J. A. Anderson, P. Lui, F. Spiga, J. A. Millan, D. C. Morse, and S. C. Glotzer, Comput. Phys. Commun. **192**, 97 (2015).
[27] See Supplemental Material http://link.aps.org/supplemental/10.1103/PhysRevLett.121.058003 for a derivation of the three-body contributions to the stress tensor and a detailed analysis of (the absence of) caging effects. The Supplemental Material includes Refs. [28–32].
[28] W. Denissen, G. Rivero, R. Nicolaÿ, L. Leibler, J. M. Winne, and F. E. Du Prez, Adv. Funct. Mater. **25**, 2451 (2015).
[29] Y.-X. Lu and Z. Guan, J. Am. Chem. Soc. **134**, 14226 (2012).
[30] J.-P. Hansen and I. R. McDonald, *Theory of Simple Liquids* (Elsevier, New York, 1990).
[31] J.-L. Barrat and J.-P. Hansen, *Basic Concepts for Simple and Complex Liquids* (Cambridge University Press, Cambridge, England, 2003).
[32] L. D. Landau and E. Lifshitz, *Theory of Elasticity*, Course of Theoretical Physics, 3rd ed. (Pergamon Press, Oxford, UK, 1986), Vol. 7.
[33] J. P. Wittmer, H. Xu, and J. Baschnagel, Phys. Rev. E **91**, 022107 (2015).
[34] I. Kriuchevskyi, J. P. Wittmer, O. Benzerara, H. Meyer, and J. Baschnagel, Eur. Phys. J. E **40**, 43 (2017).
[35] P. E. Rouse, Jr., J. Chem. Phys. **21**, 1272 (1953).
[36] F. Bomboi, F. Romano, M. Leo, J. Fernandez-Castanon, R. Cerbino, T. Bellini, F. Bordi, P. Filetici, and F. Sciortino, Nat. Commun. **7**, 13191 (2016).
[37] R. Wang, J. A. Johnson, and B. D. Olsen, Macromolecules **50**, 2556 (2017).